Article

Cell Metabolism

Hematopoietic *Kit* Deficiency, rather than Lack of Mast Cells, Protects Mice from Obesity and Insulin Resistance

Graphical Abstract

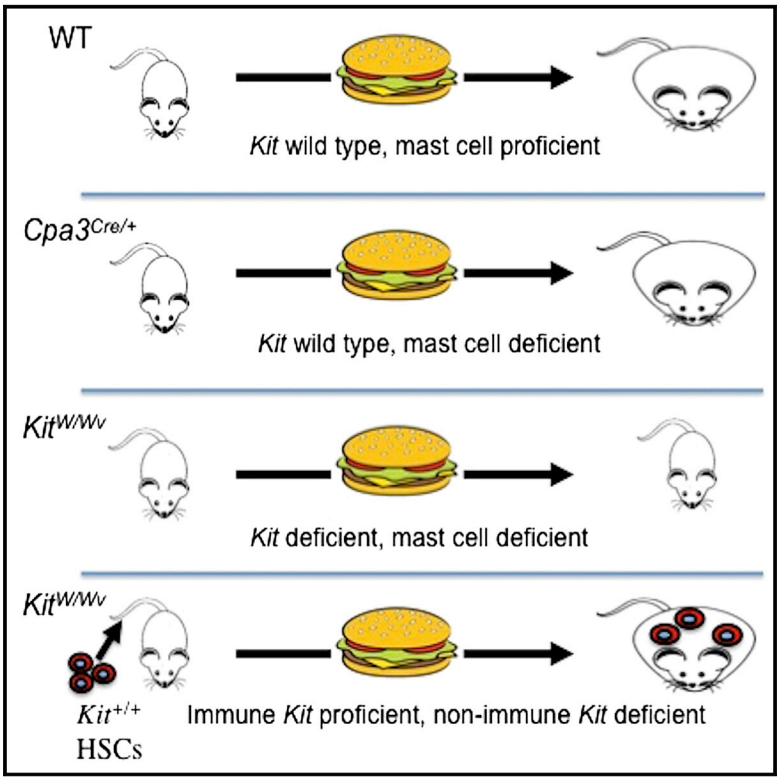

Highlights

- Obesity and insulin resistance are unaffected by mast cell deficiency
- Global *Kit* deficiency protects mice from obesity and associated metabolic disorders
- Reconstitution of *Kit* mutant mice with $Kit^{+/+}$ HSCs normalizes metabolic phenotype

Authors

Dario A. Gutierrez, Sathya Muralidhar, ..., Stephan Herzig, Hans-Reimer Rodewald

Correspondence

hr.rodewald@dkfz.de

In Brief

Mice with *Kit* mutations have several immune and non-immune abnormalities, including mast cell deficiency, and are protected from weight gain and insulin resistance during diet-induced obesity. Gutierrez et al. show that this protection is not mediated by mast cell deficiency, as previously thought, but instead through hematopoietic *Kit* deficiency.

Gutierrez et al., 2015, Cell Metabolism *21*, 678–691
May 5, 2015
http://dx.doi.org/10.1016/j.cmet.2015.04.013

CellPress

Cell Metabolism
Article

Hematopoietic *Kit* Deficiency, rather than Lack of Mast Cells, Protects Mice from Obesity and Insulin Resistance

Dario A. Gutierrez,[1] Sathya Muralidhar,[1] Thorsten B. Feyerabend,[1] Stephan Herzig,[2] and Hans-Reimer Rodewald[1,*]
[1]Division of Cellular Immunology, German Cancer Research Center, Heidelberg, D-69120, Germany
[2]Institute for Diabetes and Cancer IDC, Helmholtz Center Munich, and Joint Heidelberg-IDC Translational Diabetes Program, Heidelberg University Hospital, Ingolstädter Landstraße 1, 85764, Neuherberg, Germany
*Correspondence: hr.rodewald@dkfz.de
http://dx.doi.org/10.1016/j.cmet.2015.04.013

SUMMARY

Obesity, insulin resistance, and related pathologies are associated with immune-mediated chronic inflammation. *Kit* mutant mice are protected from diet-induced obesity and associated co-morbidities, and this phenotype has previously been attributed to their lack of mast cells. We performed a comprehensive metabolic analysis of *Kit*-dependent $Kit^{W/Wv}$ and *Kit*-independent $Cpa3^{Cre/+}$ mast-cell-deficient mouse strains, employing diet-induced or genetic ($Lep^{Ob/Ob}$ background) models of obesity. Our results show that mast cell deficiency, in the absence of *Kit* mutations, plays no role in the regulation of weight gain or insulin resistance. Moreover, we provide evidence that the metabolic phenotype observed in *Kit* mutant mice, while independent of mast cells, is immune regulated. Our data underscore the value of definitive mast cell deficiency models to conclusively test the involvement of this enigmatic cell in immune-mediated pathologies and identify *Kit* as a key hematopoietic factor in the pathogenesis of metabolic syndrome.

INTRODUCTION

The inflammatory basis for obesity-induced insulin resistance was put forth upon the discovery of elevated levels of TNF-α in adipose tissue (AT) of obese humans and diet-induced obese mice (Hotamisligil et al., 1995; reviewed in McNelis and Olefsky, 2014). Subsequently, numerous studies revealed a complex cascade of events at the intersection of both inflammatory and insulin signaling pathways. Macrophages, neutrophils, eosinophils, $CD4^+$ T cells, $CD8^+$ T cells, T regulatory cells (Treg), B cells, innate lymphoid cells (ILC) 2, and NKT cells have all been shown to be involved in the regulation of the inflammatory status of AT and other metabolic organs, and thus in the development of insulin resistance and type 2 diabetes (T2D) (reviewed in Mathis, 2013).

Recently, a positive correlation between mast cell content and hallmarks of AT inflammation in obese humans and diet-induced obese mice has been reported (Altintas et al., 2011; Divoux et al., 2012; Liu et al., 2009; Tanaka et al., 2011). This correlation prompted studies of the effects of "mast cell deficiency" on AT inflammation, insulin resistance, and T2D in diet-induced obese $Kit^{W/Wv}$ and $Kit^{W\text{-}sh/W\text{-}sh}$ mice, which revealed that *Kit* mutant mice were protected from weight gain and insulin resistance (Liu et al., 2009; Tanaka et al., 2011). Because *Kit* mutant mice are mast cell deficient, these experiments raised the intriguing possibility that lack of mast cells was underlying disease resistance.

Mast cells are classically known as effector cells for IgE-mediated allergic inflammation. Based on work in *Kit* mutant mice, a plethora of phenotypes beyond allergy has also been attributed to mast cells. These mice have, in addition to their mast cell deficiency, pleiotropic defects including abnormalities in hematological parameters (anemia, megakarocytosis, thrombocytosis), innate (neutropenia or neutrophilia and expanded myeloid derived suppressor cells [MDSCs]) and adaptive (decreased numbers of γδ T cells and Treg and increased numbers of αβ T cells) immunity, splenomegaly, lack of intestinal pacemaker cells of Cajal, deficiency of melanocytes, and cardiomegaly (Kiss et al., 2011; Maeda et al., 1992; Michel et al., 2013; Nigrovic et al., 2008; Piconese et al., 2011; Puddington et al., 1994; Russell, 1979; Waskow and Rodewald, 2002; Zhou et al., 2007). To "bypass" these manifold defects, the "mast cell knockin" technique (Kawakami, 2009; Nakano et al., 1985) was developed. This technique employs intravenous transplantation of large numbers of in vitro-generated bone-marrow-derived mast cells (BMMCs) into *Kit* mutant mice, and any phenotype reversal has been attributed to mast cell function. Indeed, upon mast cell reconstitution, *Kit* mutant mice became susceptible to the development of insulin resistance and T2D (Liu et al., 2009; Tanaka et al., 2011); hence, this phenotype was attributed to mast cells and mast-cell-dependent factors.

Kit-independent mast-cell-deficient mice have recently been generated, and alarmingly, many, if not most, re-visited "mast-cell-dependent" phenotypes have not been confirmed (Antsiferova et al., 2013; Dudeck et al., 2011; Feyerabend et al., 2011; Gomez-Pinilla et al., 2014; Gutierrez et al., 2014; Peschke et al., 2015; Rodewald and Feyerabend, 2012; Schönhuber et al., 2014; Willenborg et al., 2014). These unexpected results demonstrated that experiments in the traditional *Kit* mutant models, even in combination with mast cell transplantation, are unreliable. Hence, it is mandatory to revisit previously claimed mast-cell-dependent phenotypes in *Kit*-independent mast-cell-deficient mice. Despite lack of such independent

confirmation, mast cells have been functionally linked to obesity and insulin resistance in over 30 reviews since the original publication by Liu et al. (2009), and consequently mast cell-stabilization has been proposed as a novel medication for obesity and diabetes (Wang and Shi, 2011). Given the implications and therapeutic potential of mast cell inhibition on these widespread diseases, we now separated effects of *Kit* deficiency from mast cell deficiency on obesity and its associated co-morbidities. Metabolic phenotyping of the *Kit*-dependent $Kit^{W/Wv}$ and *Kit*-independent $Cpa3^{Cre/+}$ mast-cell-deficient mice during diet-induced or genetic ($Lep^{Ob/Ob}$ background) obesity revealed that mast cell deficiency alone plays no role in the regulation of weight gain, insulin resistance, or T2D. Instead, the metabolic phenotype of *Kit* mutant mice, while independent of mast cells, is immune regulated, which identifies *Kit* as a key hematopoietic gene in the pathogenesis of metabolic syndrome.

RESULTS

Mast Cell Deficiency Does Not Protect Mice from Obesity and Insulin Resistance

$Cpa3^{Cre/+}$ mice are wild-type for *Kit* ($Kit^{+/+}$) but are constitutively mast cell deficient due to the genotoxicity of strong Cre recombinase expression from the *Cpa3* locus in mast cells. Besides their mast cell deficiency and a reduction of basophils, $Cpa3^{Cre/+}$ mice present no other known immunological or non-immunological abnormalities (Feyerabend et al., 2011). To separate the potential roles of mast cells from the effects of *Kit* mutations in this disease, we placed mast-cell-deficient C57BL/6 (B6.$Cpa3^{Cre/+}$) mice or mast-cell-proficient littermate controls (B6.$Cpa3^{+/+}$) on a high-fat diet (HFD) (60% kcal from fat; 35% fat content) for 16 weeks. Surprisingly, when compared to mice fed normal chow (low-fat diet [LFD]; 6% fat content), both B6.$Cpa3^{Cre/+}$ and B6.$Cpa3^{+/+}$ mice showed identical weight gain (Figure 1A). After 16 weeks of HFD feeding, body composition assessed by ECHO-MRI revealed no effects of mast cell deficiency on total AT (Figure 1B) or total lean mass (Figure S1A). In support of this, epididymal (Figure 1C) and perirenal AT mass (Figure S1B) were comparable in B6.$Cpa3^{Cre/+}$and B6.$Cpa3^{+/+}$ mice. Likewise, liver and spleen weight were unaffected by mast cell deficiency (Figures S1C and S1D).

Next, we investigated the abundance of mast cells in AT before and after HFD-induced obesity. In agreement with earlier reports (Liu et al., 2009; Tanaka et al., 2011), both frequencies (Figures 1D and 1E) and absolute numbers (not shown) of mast cells were increased in obese compared to lean B6.$Cpa3^{+/+}$ AT, whereas obese B6.$Cpa3^{Cre/+}$mice remained fully mast-cell-deficient based on flow cytometric analysis for mast cells (defined as $CD45^+IgE^+CD117^+$ cells) (Figure 1D) and on expression of the mast-cell-specific marker genes *Cpa3* (data not shown) and *Cma1*, which encodes Chymase 1 (Figure 1E). Histological analysis of AT confirmed the increased mast cell density in obese compared to non-obese B6.$Cpa3^{+/+}$ mice, while mast cells were absent in both obese and non-obese B6.$Cpa3^{Cre/+}$ tissues (Figure 1F). Collectively, mast cells are induced in obese fat tissue in wild-type mice but remain undetectable in B6.$Cpa3^{Cre/+}$ mice regardless of feeding conditions. Given that weight gain was indistinguishable between B6.$Cpa3^{+/+}$ and B6.$Cpa3^{Cre/+}$ mice, we conclude that lack of mast cells does not prevent diet-induced obesity.

To probe the potential role of mast cells in a genetic model of obesity, we generated B6.$Lep^{Ob/Ob}Cpa3^{Cre/+}$mice that, in addition to their mast cell deficiency, lack leptin. B6.$Lep^{Ob/Ob}Cpa3^{Cre/+}$ mice were compared to their mast-cell-proficient B6.$Lep^{Ob/Ob}Cpa3^{+/+}$ as well as to their lean B6.$Lep^{Ob/+}Cpa3^{+/+}$ and B6.$Lep^{Ob/+}Cpa3^{Cre/+}$ littermates (Figures 1G–1J). Of note, as in the diet-induced model, mast cell frequencies were elevated in obese compared to lean controls, and this increase was only observed in B6.$Lep^{Ob/Ob}Cpa3^{+/+}$ and not in B6.$Lep^{Ob/Ob}Cpa3^{Cre/+}$ mice (Figure 1J). In this model, in support of the diet-induced obesity studies, mast cell deficiency did not affect weight gain (Figure 1G), total adiposity (Figure 1H), or epididymal AT mass (Figure 1I).

After HFD feeding in the B6.$Cpa3^{Cre/+}$ and B6.$Cpa3^{+/+}$ mice, numbers of total $CD45^+$ leukocytes were increased in visceral AT (Figure 2A). This increase in cell numbers was paralleled by elevated absolute numbers of macrophages (Figure 2B). Cellular dissection of the $CD45^+$ compartment showed a slight increase in the proportions of macrophages and decreases in proportions of eosinophils and B cells, while proportions of T cells remained unaffected by HFD feeding (Figures 2C–2F). Within the T cell compartment, proportions of total $CD4^+$ T cells and Treg were unchanged, while proportions of $CD8^+$ T cells were elevated (Figures 2G–2I) after HFD feeding. All of these parameters reflect the expected responses to HFD feeding; however, none of these populations were affected by mast cell deficiency (Figures 2A–2I).

Epididymal AT (Figures 2J–2M), liver and muscle (Figures S2A–S2H) from LFD- or HFD-fed B6.$Cpa3^{Cre/+}$ and B6.$Cpa3^{+/+}$ mice were analyzed for mRNA expression of inflammatory markers. The cytokine TNF-α is one of the main mediators of AT inflammation and insulin resistance (Uysal et al., 1997), and mast cells can produce TNF-α (Gordon and Galli, 1990); however, the HFD-feeding-associated increase in *Tnf* mRNA expression in AT was mast cell independent (Figure 2J). Similarly, the upregulated expression by HFD feeding of the macrophage marker *Emr1* (also known as F4/80) (Figure 2K) and the monocyte/macrophage chemoattractant and inflammatory cytokine *Ccl2* (Figure 2L) were unaffected by mast cell deficiency. Expression of *Il6* in AT tissue was not increased by HFD-feeding but was significantly higher in LFD-fed B6.$Cpa3^{Cre/+}$ mice in comparison to their LFD B6.$Cpa3^{+/+}$ littermate controls (Figure 2M), the relevance of which remains to be determined. The expression of these inflammatory markers was also assessed in liver and muscle, and with the exception of *Il6* expression in muscle of lean mice, mast cell deficiency had no effects on these parameters (Figures S2A–S2H). In contrast to AT tissue, numbers of mast cells were not increased (muscle) or induced (liver) in response to HFD, and they remained undetectable in B6.$Cpa3^{Cre/+}$ mice (Figures S2I–S2L).

Glucose homeostasis and insulin resistance during diet-induced obesity were assessed by glucose tolerance tests (GTTs) (Figure 2N), fasting plasma insulin (Figure 2O), circulating plasma insulin 45 and 120 min post glucose bolus injection (Figures S1E and S1F), and Serine-473 Akt phosphorylation in epididymal AT (Figures S1G and S1H), gastrocnemius muscle, and liver (data not shown) 15 min post-insulin

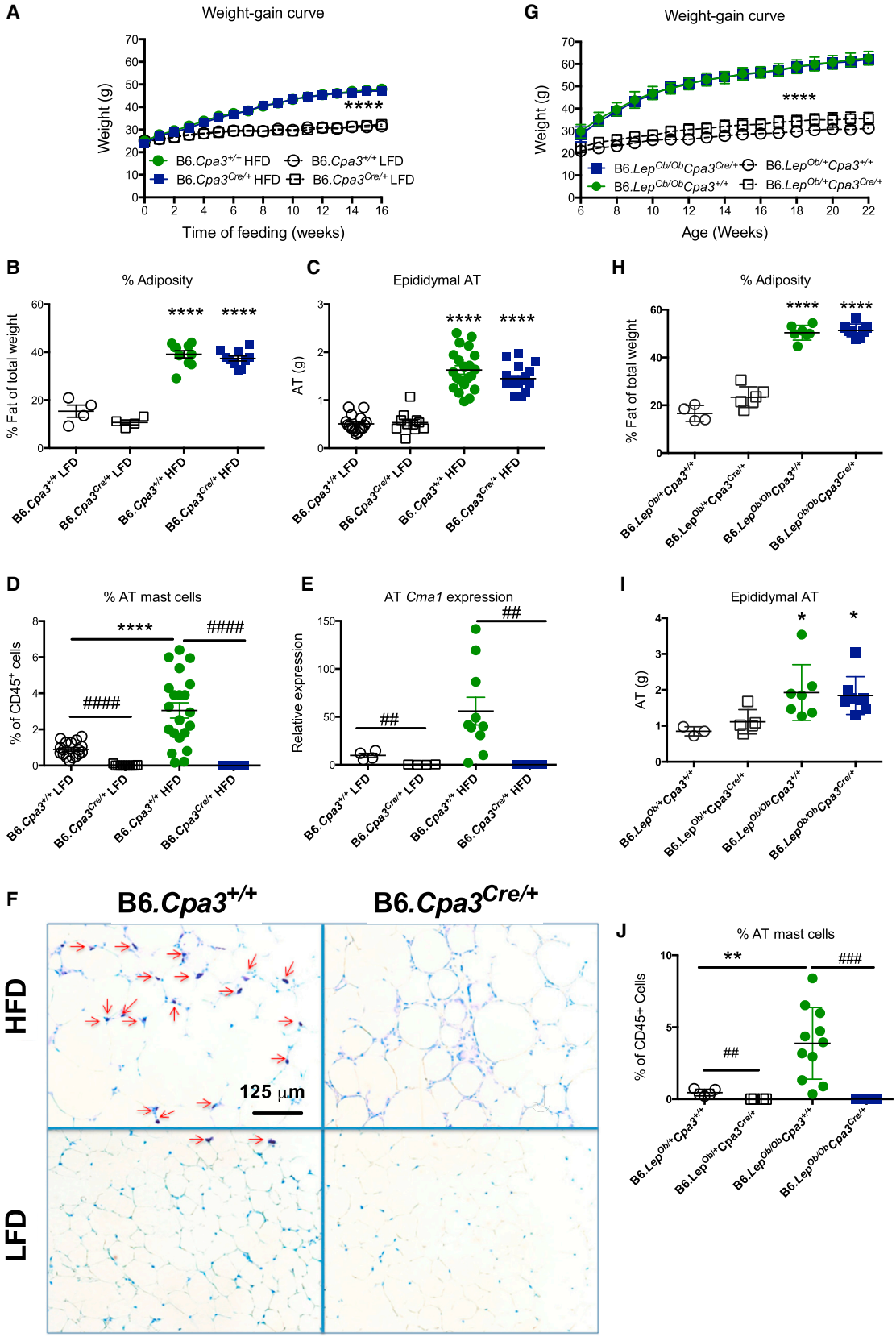

(legend on next page)

bolus injection. Mast cell deficiency did not affect glucose homeostasis, insulin resistance, or T2D. Moreover, mast cell deficiency did not affect glucose tolerance (Figure 2P) or fasting insulin levels (Figure 2Q) in the leptin-deficient obese model. Finally, pharmacological inhibition of mast cell degranulation with disodium chromoglycate (DSCG) had no effect on weight gain in HFD-fed mast cell-proficient, or -deficient mice (Figure 2R).

Kit Deficiency Protects Mice from Diet-Induced Obesity and Metabolic Syndrome

To address the impact of *Kit* mutations on obesity and the metabolic syndrome, we dissociated mast cell deficiency from *Kit* deficiency in WB × C57BL/6 (WBB6F1) mice, which is the historical background strain of all experiments using $Kit^{W/Wv}$ mice, including the reported metabolic studies (Liu et al., 2009; Tanaka et al., 2011). We generated WBB6F1.$Kit^{+/+}$ $Cpa3^{+/+}$ (*Kit* wild-type; mast cell-proficient) (termed $Cpa3^{+/+}$ below), WBB6F1.$Kit^{+/+}Cpa3^{Cre/+}$ (*Kit* wild-type; mast cell deficient) (termed $Cpa3^{Cre/+}$ below), and WBB6F1.$Kit^{W/Wv}Cpa3^{+/+}$ (severely impaired Kit signaling due to the compound *Kit* mutations; mast cell deficient) (termed $Kit^{W/Wv}$ below). Breedings were set up to generate sufficient numbers of littermates for side-by-side comparisons.

At 8 weeks of age, before the start of HFD feeding, mice of all genotypes had similar body mass (Figure 3A); however, $Kit^{W/Wv}$ mice were hyperglycemic in comparison to both $Cpa3^{+/+}$ and $Cpa3^{Cre/+}$ mice (Figure 3B). In agreement with previous reports (Liu et al., 2009; Tanaka et al., 2011), when placed on an HFD, $Kit^{W/Wv}$ mice failed to gain weight, while both mast cell-proficient $Cpa3^{+/+}$ and mast-cell-deficient $Cpa3^{Cre/+}$ littermate controls showed indistinguishable weight gain curves (Figure 3C; see Figure S3A for comparison to LFD controls). No differences were found in food intake between groups (data not shown). Body composition analyses by ECHO-MRI after 16 weeks of HFD-feeding showed a >2-fold reduction in percent adiposity, as well as a significant reduction in total lean mass in the $Kit^{W/Wv}$ when compared to $Cpa3^{+/+}$ and $Cpa3^{Cre/+}$ mice (Figures 3D and 3E). Upon tissue collection, $Kit^{W/Wv}$ mice had a 3-fold lower epididymal (Figure 3F) and perirenal AT mass (Figure S3B) compared to $Cpa3^{+/+}$ and $Cpa3^{Cre/+}$ mice. AT of $Cpa3^{Cre/+}$ and $Kit^{W/Wv}$ mice remained fully mast cell deficient (Figure 3G). The proportions of macrophages from total $CD45^+$ cells were not changed between groups (Figure S3C); however, absolute macrophage numbers (Figure S3D), percent eosinophils (Figure S3E), and percent T cells (Figure S3F) were significantly affected in the $Kit^{W/Wv}$ mice. The proportions of $CD8^+$ and $CD4^+$ cells within the T cell compartment were not changed in either group (Figures S3G and S3H).

While $Cpa3^{+/+}$ and $Cpa3^{Cre/+}$ mice displayed the expected normal response to HFD feeding, $Kit^{W/Wv}$ mice showed alterations in lipid profiles, glucose tolerance, and insulin resistance during obesity. $Kit^{W/Wv}$ mice presented hypertriglyceridemia and reduced fasting total plasma cholesterol levels (Figures 3H and 3I) after 16 weeks of HFD feeding; however, $Cpa3^{Cre/+}$ mice were not different from $Cpa3^{+/+}$ mice; hence, these changes in lipid profiles are mast cell independent. Assessment of glucose tolerance (Figure 3J), fasting plasma insulin (Figure S3I), and plasma insulin 30 min after glucose bolus injection (Figure S3J) confirmed that $Kit^{W/Wv}$ mice are protected from diet-induced glucose intolerance and insulin resistance (Liu et al., 2009; Tanaka et al., 2011). However, this protection in WBB6F1 mice is not mediated by mast cells because *Kit*-independent mast-cell-deficient $Cpa3^{Cre/+}$ mice lacked this resistance.

Profound Effects of *Kit* Deficiency on White AT mRNA Transcriptome

We compared global gene expression patterns in AT from $Kit^{W/Wv}$ mice versus $Cpa3^{Cre/+}$ or $Cpa3^{+/+}$ mice under either LFD or HFD feeding conditions. Total RNA was collected from epididymal AT of $Kit^{W/Wv}$, $Cpa3^{Cre/+}$, and $Cpa3^{+/+}$ mice fed either a LFD or HFD for 12 weeks (Figure S3A), and gene expression was examined by whole-transcriptome microarray analysis. After normalization using the quantile method, data were visualized using a principal component analysis. As shown in Figure 4A, the largest component of variance is represented in the x axis (PC1), which corresponds to HFD feeding (black oval) versus LFD feeding (red rectangle).

Of note, $Kit^{W/Wv}$ mice, despite HFD feeding (red dots), fell into the LFD group (red rectangle in Figure 4A), strongly

Figure 1. Weight Gain, Glucose Tolerance, and Insulin Resistance Are Unaffected by Mast Cell Deficiency in Models of Diet- and Genetic-Induced Obesity

(A–F) Male 8-week-old B6.$Cpa3^{Cre/+}$ mice and their B6.$Cpa3^{+/+}$ littermate controls were placed on a LFD or HFD and their weights were tracked weekly for 16 weeks. (n = 11–21 per group).

(B) Percent adiposity (total fat/total body mass) determined by ECHO-MRI.

(C) Epididymal AT mass.

(D) Mast cell content in epididymal AT assessed by flow cytometry. Percentage of CD117 $(Kit)^+IgE^+$ mast cells from total $CD45^+$ cells.

(E) mRNA expression of *Cma1* in epididymal AT.

(F) Metachromatic mast cells (red arrows) visualized in paraffin embedded epididymal AT by toluidine blue staining; images are from one experiment representative of three independent experiments.

(G–J) The weights of male B6.$Lep^{Ob/Ob}Cpa3^{Cre/+}$ mast-cell-deficient mice and their B6.$Lep^{Ob/Ob}Cpa3^{+/+}$, B6.$Lep^{Ob/+}Cpa3^{Cre/+}$, and B6.$Lep^{Ob/+}Cpa3^{+/+}$littermate controls, all kept on a LFD, were tracked weekly between 6 and 22 weeks of age (n = 4–8).

(H) Percent adiposity.

(I and J) (I) Epididymal AT mass and (J) mast cell content in epididymal AT of genetically obese leptin-deficient mice assessed as described above.

Data are shown as mean ± SEM and are pooled from two or three independent experiments.

Each dot in the dot plots represents one individual mouse. One-way ANOVA or two-way ANOVA with a Tukey's post hoc test (weight gain curves) were used to calculate statistical differences. $^*p < 0.05$; $^{**}p < 0.01$; $^{****}p < 0.0001$ between obese (diet induced or genetic) and their corresponding lean controls. $^{\#\#}p < 0.01$; $^{\#\#\#\#}p < 0.0001$ between mast-cell-deficient B6.$Cpa3^{Cre/+}$ and their respective mast-cell-proficient B6.$Cpa3^{+/+}$ littermate controls.

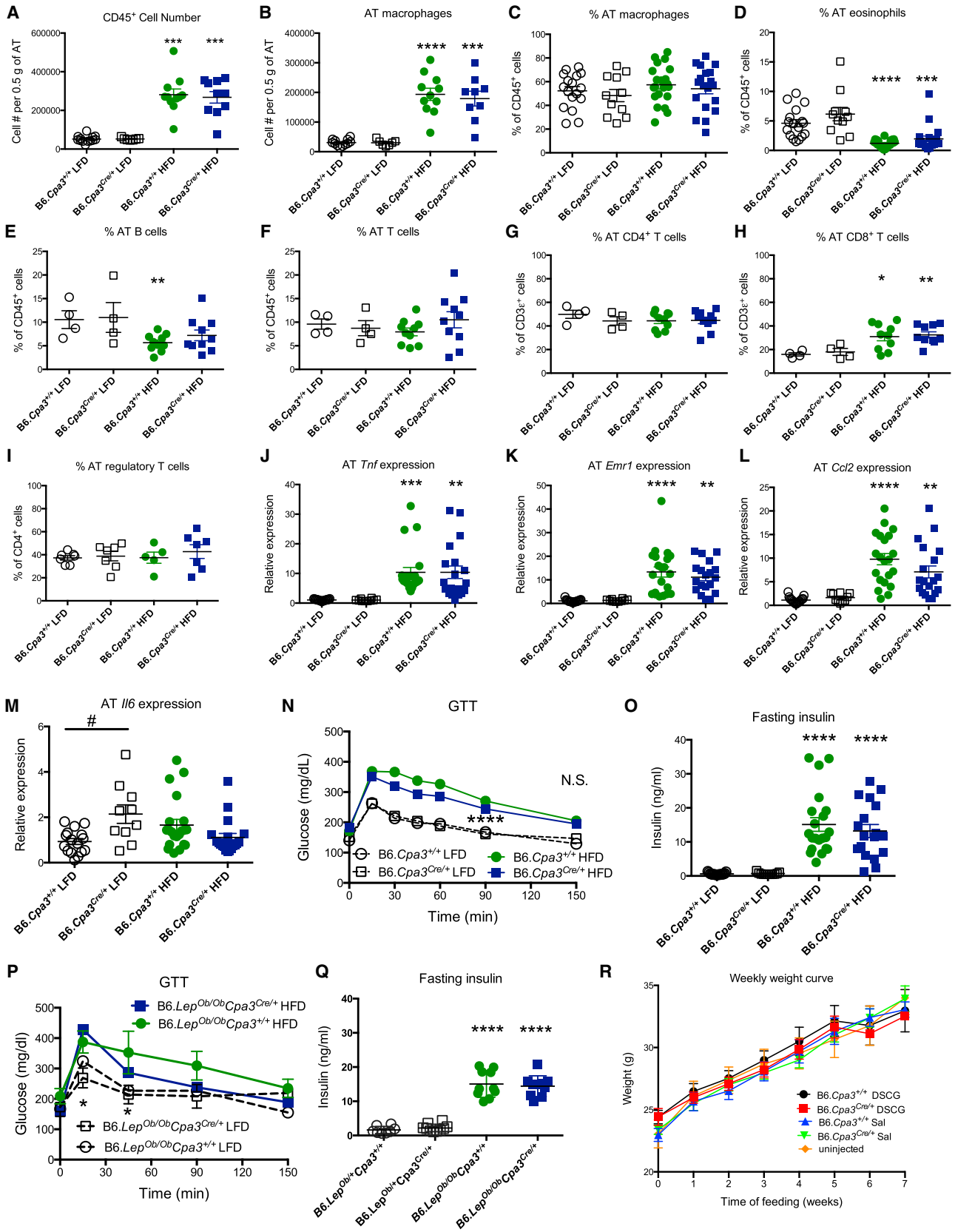

(legend on next page)

suggesting that $Kit^{W/Wv}$ mice lack the normal response to HFD feeding. To analyze the impact of *Kit* deficiency on global gene expression under HFD feeding conditions, we compared $Kit^{+/+}$ (regardless of whether they have a $Cpa3^{+/+}$ or $Cpa3^{Cre/+}$ genotype) to $Kit^{W/Wv}$ mice; we found that 2,190 genes were significantly differentially regulated in AT by the *Kit* mutation (heatmap shown in Figure 4B). A graphical fold-change comparison displays the 15 most highly differentially expressed genes between $Kit^{+/+}$ and $Kit^{W/Wv}$ HFD-fed mice (Figure 4C). Further analysis identified the strongest differences in gene expression comparing LFD- and HFD-fed Kit wild-type mice in genes that were typically upregulated (i.e., *Tph2*, *Trem2*, *Itgad*, and *Gpnmb*) or downregulated (i.e., *Acsm3* and *Pck1*) in AT with obesity (Figure 4D). Strikingly, the pattern of differential gene expression comparing LFD- versus HFD-fed wild-type mice (Figure 4D) resembled that of HFD-fed $Kit^{+/+}$ versus HFD-fed $Kit^{W/Wv}$ mice (Figure 4C), providing further evidence that *Kit* mutant mice placed on a HFD remain on a metabolically ''lean'' gene expression program.

$Kit^{+/+}$ Bone Marrow Transplantation into *Kit* Mutant Mice Reverses the Immune and Metabolic Phenotype without Rescue of the Gut Motility Defect

Kit mutant mice suffer from many mast-cell-independent immune abnormalities described above. Additionally, they have marked defects outside of the immune system, including lack of cells of Cajal, which impairs gut motility (Huizinga et al., 1995; Maeda et al., 1992; Reber et al., 2012; Sergeant et al., 2002), the development of spontaneous stomach ulcers (Shimada et al., 1980), forestomach papillomas (Kitamura et al., 1980), abnormal liver function (Magnol et al., 2007), and insulin secretion from β cells (Feng et al., 2012), which could all affect the metabolic phenotype of these mice. Therefore, we addressed by bone marrow transplantation whether defects in hematopoietic or non-hematopoietic Kit expression were underlying the resistance of *Kit* mutant mice to obesity. WBB6F1.$Kit^{W/Wv}$ mice accept syngeneic $Kit^{+/+}$ hematopoietic stem cells (HSCs) without irradiation (Waskow et al., 2009 and references therein), resulting in an adult hematopoietic system of donor ($Kit^{+/+}$) origin (Figure S4; data not shown). Engrafted mice showed reversal of all the *Kit*-mutation-dependent abnormalities tested, including normalized hematocrit (Figure 5A), increased ILC3 levels, and normalized intraepithelial TCR $\gamma\delta^+$ and TCR $\alpha\beta^+$ T cells (data not shown). In contrast, bone marrow transplantation could not reverse the gut motility defect associated with lack of cells of Cajal (Figure 5B), despite contrary reports (Ishii et al., 2009). We also reconstituted WBB6F1.$Kit^{W/Wv}$ mice with WBB6F1.$Cpa3^{Cre/+}$ bone marrow, which led to completely normalized stem and progenitor cell compartments (Figure S4B; data not shown), and that of all other tested *Kit* mutation-dependent immune abnormalities except for mast cells (analyzed in peritoneal cavity and AT; data not shown).

Despite the major non-immunological abnormalities that cannot be overcome by hematopoietic reconstitution, $Kit^{+/+}$ HSC transplantation reversed all analyzed metabolic phenotypes of $Kit^{W/Wv}$ mice; that is, it normalized base line hyperglycemia (Figure 5C), weight gain during HFD-feeding (Figure 5D), and loss of protection from glucose intolerance (Figure 5E). The rescue was similar in mice reconstituted with wild-type ($Cpa3^{+/+}$) or mast-cell-incompetent ($Cpa3^{Cre/+}$) bone marrow. Bone marrow transplantation also normalized total AT mass, epididymal AT mass, and total lean mass after HFD feeding (Figures 5F–5H).

Kit-Mutation-Dependent Metabolic Defects Are Not Replicated by Absence or Perturbations in Immune Lymphoid Lineages

One of the main immune phenotypes associated with *Kit* mutations is abnormal lymphopoiesis that includes abnormal T cell development in the thymus (Waskow et al., 2002; Waskow and Rodewald, 2002), reduced Treg cells (Piconese et al., 2011), decreased intraepithelial TCR $\gamma\delta^+$ T cells and increased numbers of intraepithelial TCR $\alpha\beta^+$ T cells in the gut (Puddington et al., 1994), and reduced levels of ILC3s (Chappaz et al., 2010; Kiss et al., 2011). The potential impact of perturbations in lymphoid lineages on the metabolic phenotype was examined in B6.$Rag2^{-/-}$mice, which completely lack mature B and T cells and have increased ILC3 levels, and in B6.$Il7r^{-/-}$ mice that lack the receptor for the key lymphopoietic factor IL-7, and thus have severe immunodeficiencies in T and B cell and innate lymphoid lineages. The metabolic phenotype of these mutants was compared to wild-type mice (B6.$Il7r^{+/-}$ littermate controls of the B6.$Il7r^{-/-}$ mice). In contrast to the *Kit* mutation-dependent phenotype, B6.$Rag2^{-/-}$ and B6.$Il7r^{-/-}$ mice had normal or even increased (former) weight gain in

Figure 2. Mast Cell Deficiency Does Not Affect AT Immune Infiltration or Inflammatory Status

(A–O) Immunological and metabolic parameters of B6 mice with or without mast cells after 16 weeks of LFD or HFD feeding.

(A–F) (A) Absolute numbers of $CD45^+$ leukocytes and (B) $CD11b^+F4/80^+$ macrophages per 0.5 g of AT. Percentages of $CD11b^+F4/80^+$ macrophages (C), $CD11b^{low}F4/80^{low}$Siglec-F^+ eosinophils (D), $CD19^+CD3\varepsilon^-$ B cells (E), and $CD3\varepsilon^+CD19^-$ T cells from total $CD45^+$ cells (F).

(G–I) Percentages of $CD4^+$ T cells (G) and $CD8^+$ T cells (H) from total $CD3\varepsilon^+$ T cells. Percentage of $Foxp3^+$ Treg from total $CD4^+$ T cells (I).

(J–M) Total RNA was isolated from epididymal AT, and the expression of inflammatory genes was assessed by quantitative real-time PCR. Expression of *Tnf* (J), *Emr1* (K), *Ccl2* (L), and *Il6* (M) in epididymal AT.

(N) GTT performed at 14 weeks of diet feeding (n = 11–21).

(O) Fasting plasma insulin after 16 weeks of HFD feeding.

(P and Q) Metabolic analyses of leptin-deficient mice with and without mast cells.

(P) GTT performed at 19 weeks of age (n = 4–8).

(Q) Fasting plasma insulin at 22 weeks of age.

(R) Male 8-week-old B6.$Cpa3^{Cre/+}$ mice and their B6.$Cpa3^{+/+}$ littermate controls were placed on HFD for 7 weeks and injected daily with 25 mg/kg DSCG or saline, and their weights were tracked weekly; an additional control group was not injected (n = 4–10).

Data are shown as mean ± SEM and are pooled from three independent experiments (DSCG study: one experiment); each dot represents one individual mouse. Statistics were performed as described for Figure 1 above. $^*p < 0.05$; $^{**}p < 0.01$; $^{***}p < 0.001$; $^{****}p < 0.0001$ between obese mice and their respective lean controls (diet or leptin effect). $^{\#}p < 0.01$ between B6.$Cpa3^{Cre/+}$ and their respective B6.$Cpa3^{+/+}$ littermate controls in the same diet ($Cpa3^{Cre/+}$ genotype effect).

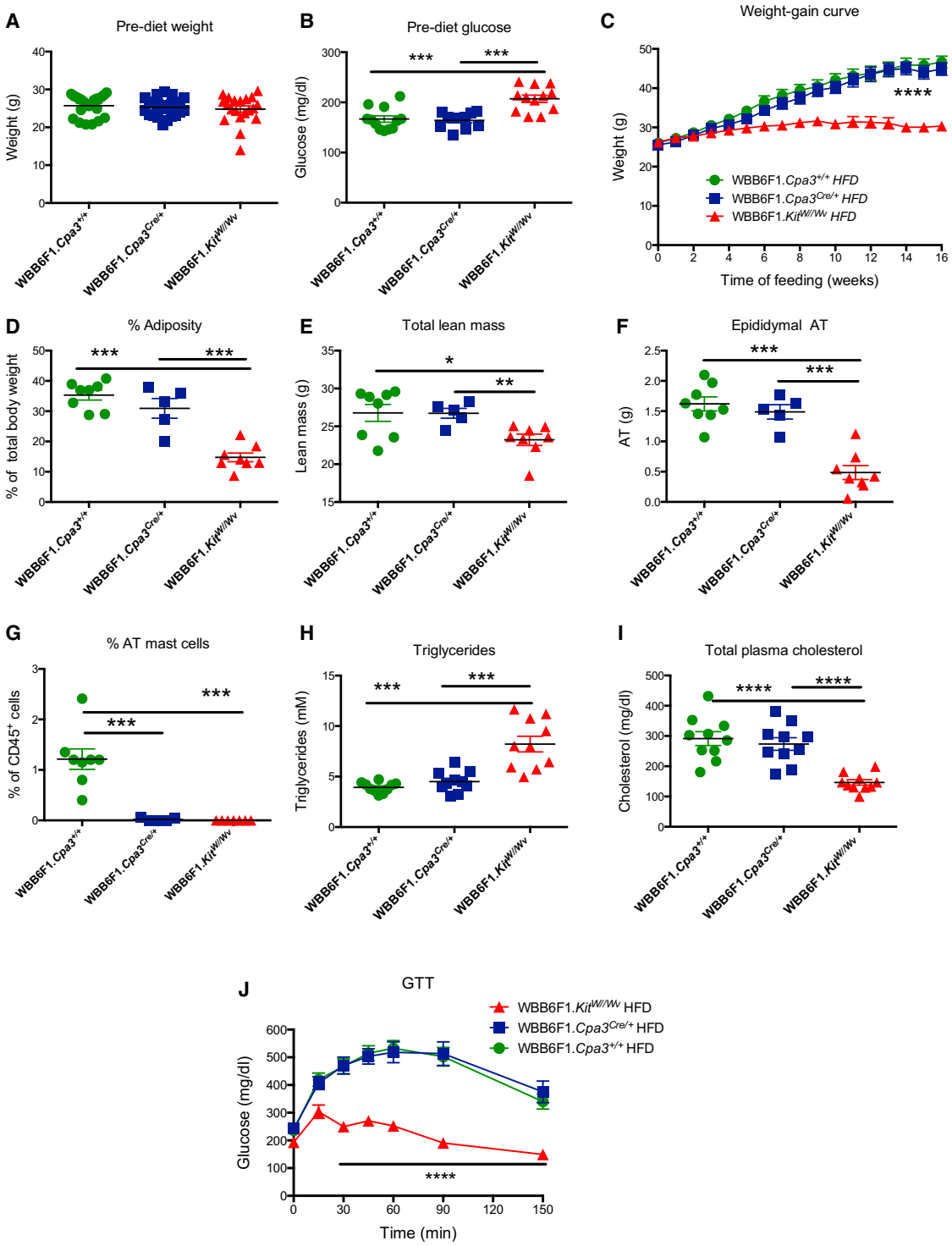

Figure 3. *Kit* Deficiency Protects from Diet-Induced Obesity and Insulin Resistance

WBB6F1.*Kit*$^{W/Wv}$, WBB6F1.*Cpa3*$^{+/+}$, and WBB6F1.*Cpa3*$^{Cre/+}$ mice were used to dissect the effects of *Kit* deficiency versus mast cell deficiency during diet-induced obesity.

(A and B) (A) Total body mass and (B) fasting plasma glucose of 8-week-old male mice were assessed before HFD feeding.

(C) Mice were placed on an HFD for 16 weeks starting at 8-weeks of age and their weights tracked weekly.

(D and E) (D) Adiposity (total fat mass/total body mass) and (E) total lean mass after 16 weeks of HFD feeding measured by ECHO-MRI.

(F) Epididymal AT mass.

(G) Mast cell content in epididymal AT shown as the percentage of total CD45^{+} cells.

(legend continued on next page)

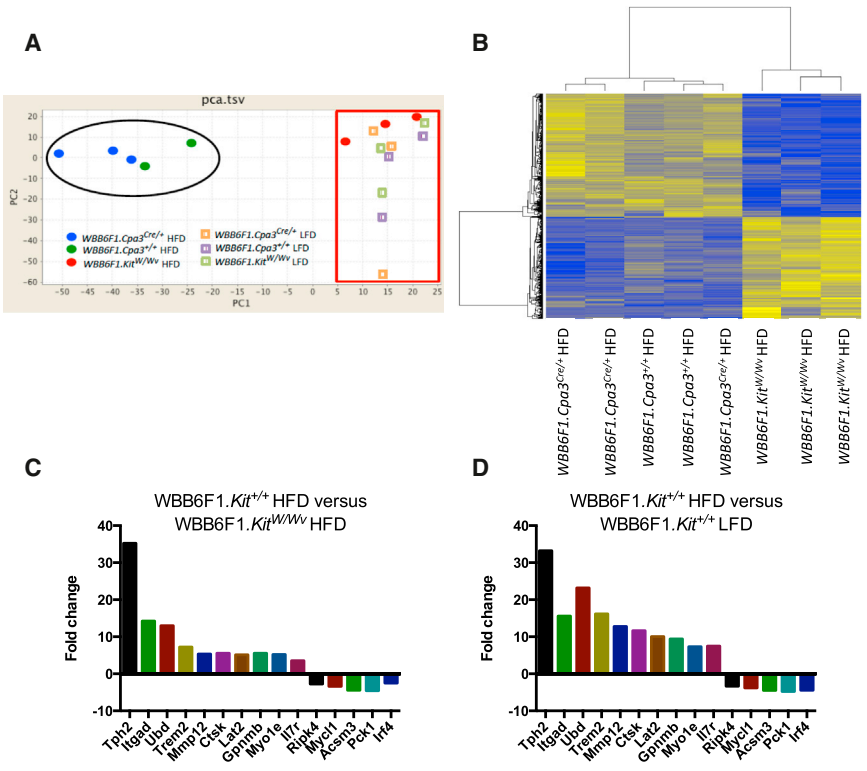

Figure 4. *Kit* Deficiency Leads to Profound Differences in Epididymal AT Gene Expression during Diet-Induced Obesity

WBB6F1.$Kit^{W/Wv}$, WBB6F1.$Cpa3^{+/+}$, and WBB6F1.$Cpa3^{Cre/+}$ mice were placed on a LFD or HFD for 12 weeks, and total RNA from their epididymal AT was isolated for microarray analysis.

(A) Data were visualized using a principal component analysis; black oval represents HFD-fed mice and red rectangle LFD-fed mice, with the exception of $Kit^{W/Wv}$ mice fed a HFD, which fell into the LFD-fed group. Gene expression differences between $Kit^{W/Wv}$, $Cpa3^{+/+}$, and $Cpa3^{Cre/+}$ mice fed a HFD were assessed by a multiple-group Empirical Bayes statistical test

(B) Genes found to be significantly downregulated or upregulated between $Kit^{W/Wv}$, $Cpa3^{+/+}$, and $Cpa3^{Cre/+}$ mice are shown in a dendrogram/heat map hybrid form.

(C and D) Bar graph comparison of the fold-change between the most significantly upregulated and downregulated genes in (C) HFD-fed $Kit^{+/+}$ mice ($Cpa3^{+/+}$ and $Cpa3^{Cre/+}$) in comparison to HFD-fed $Kit^{W/Wv}$ mice and in (D) HFD-fed $Kit^{+/+}$ mice ($Cpa3^{+/+}$ and $Cpa3^{Cre/+}$) in comparison to LFD-fed $Kit^{+/+}$ mice ($Cpa3^{+/+}$ and $Cpa3^{Cre/+}$).

Data are from one experiment with n = 2 to 3 per group.

comparison to the controls when fed a HFD (Figure 6A). Unlike *Kit* mutant mice, lymphoid-deficient mice were not protected from glucose intolerance (Figure 6B), and epididymal AT mass was also unaffected (Figure 6C). The relative increase in the percentages of $CD11b^{+}F4/80^{+}$ macrophages among total $CD45^{+}$ cells in the epididymal AT of B6.$Rag2^{-/-}$ and B6.$Il7r^{-/-}$ mice when compared to B6.$Il7r^{+/-}$ controls (Figure 6D) was likely due to the lack/reduction of lymphocytes, as the absolute number of macrophages per gram of AT was not increased, but instead trended toward a reduction in these mutants (Figure 6E). As expected, T (Figures 6F–6H) and B cells (Figures 6F, 6I, and 6J) were completely absent in B6.$Rag2^{-/-}$ mice and severely reduced in B6.$Il7r^{-/-}$ mice when compared to the controls. Collectively, it is unlikely that lymphoid perturbations alone are responsible for the protection from obesity found in *Kit* mutant mice. Due to the complexity of the hematopoietic phenotypes observed in these mutants, new approaches may be required in the future to definitively pinpoint the cellular or molecular defects underlying the protection of *Kit* mutants to obesity and T2D.

DISCUSSION

Obesity is associated with a state of chronic inflammation that contributes to the concomitant development of an insulin-resistant pre-diabetic state that leads to T2D (Hill et al., 2014; Hotamisligil and Erbay, 2008). Many immune cells play at least a minimum role in the pathogenesis of obesity (Eheim et al., 2014; Mraz and Haluzik, 2014), underlining the potential relevance of multiple hematopoietic lineages for these diseases. The receptor tyrosine kinase Kit is expressed in the hematopoietic system in many cell types including stem and progenitor cells, mast cells, and ILCs, and it plays important roles in hematopoietic development and homeostasis. Mice with mutations at the *Kit* locus ($Kit^{W/Wv}$, $Kit^{W\text{-}sh/W\text{-}sh}$) are protected from weight gain, metabolic chronic inflammation, insulin resistance, and T2D when challenged with HFD feeding. Since *Kit* mutant mice lack mast cells, this protection was attributed to the lack of mast cells (Liu et al., 2009; Tanaka et al., 2011). In this study we showed that the protective phenotype against these diseases is linked to hematopoietic *Kit* deficiency rather than mast cell deficiency.

We have demonstrated the mast cell independence of weight gain and T2D in three models: (1) In the C57BL/6 background, mast-cell-deficient $Cpa3^{Cre/+}$ mice were studied side-by-side with mast-cell-proficient $Cpa3^{+/+}$ littermate controls. (2) We compared leptin-deficient obese mice with (B6.$Lep^{Ob/Ob}$ $Cpa3^{+/+}$) or without (B6.$Lep^{Ob/Ob}Cpa3^{Cre/+}$) mast cells. (3) In the $Kit^{W/Wv}$ strain, we used the $Cpa3^{Cre}$ allele to dissociate the effects of the *Kit* mutation from the effect of lack of mast cells. The

(H and I) (H) Fasting plasma triglycerides and (I) total cholesterol after 16 weeks of HFD-feeding.

(J) GTT was performed at 14 weeks of HFD feeding.

Data are represented as mean ± SEM and are pooled from three independent experiments. Each symbol in the dot plots represents one individual mouse for weight gain curve and GTT (n = 8–12 mice per group). Statistics were performed as described for Figure 1 above. *p < 0.05; **p < 0.01; ***p < 0.001; ****p < 0.0001, between WBB6F1.$Cpa3^{+/+}$ and WBB6F1.$Cpa3^{Cre/+}$ HFD groups versus WBB6F1.$Kit^{W/Wv}$ HFD group (*Kit* mutation effect).

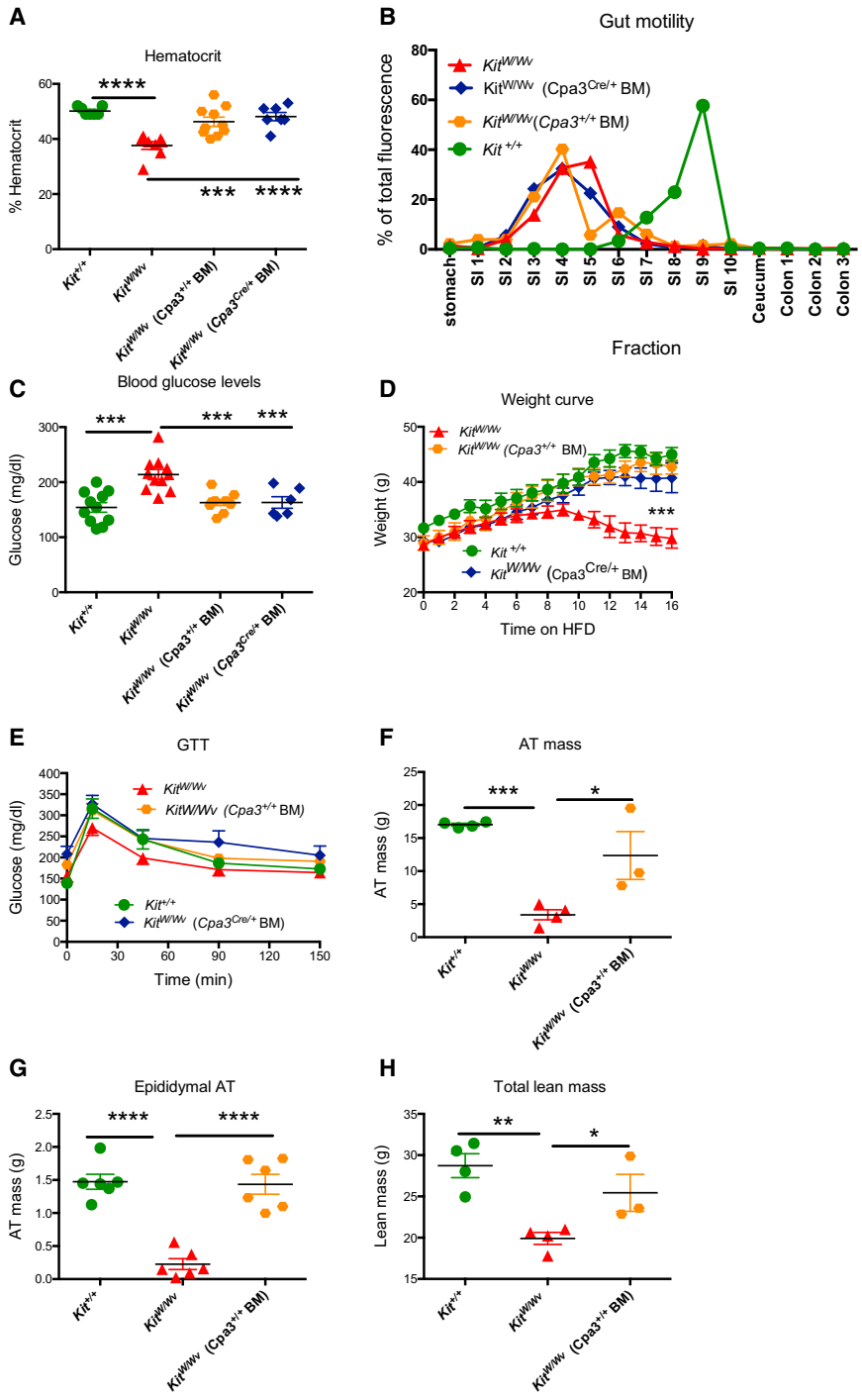

Figure 5. *Kit*$^{+/+}$ Bone Marrow Reconstitution of *Kit*$^{W/Wv}$ Mice Reverses the Metabolic Phenotype

WBB6F1.*Kit*$^{W/Wv}$ (*Kit*$^{W/Wv}$) mice were transplanted with either WBB6F1.*Kit*$^{+/+}$*Cpa3*$^{+/+}$ (*Cpa3*$^{+/+}$) or WBB6F1.*Cpa3*$^{Cre/+}$ (*Cpa3*$^{Cre/+}$) bone marrow; mice were analyzed or placed on a HFD 6 weeks after transplantation.

(A) Hematocrit of *Kit*$^{+/+}$ and *Kit*$^{W/Wv}$ mice without transplantation, and that of *Kit*$^{W/Wv}$ mice transplanted with *Kit*$^{+/+}$ (*Kit*$^{W/Wv}$ (*Cpa3*$^{+/+}$ BM)), or with *Cpa3*$^{Cre/+}$ (*Kit*$^{W/Wv}$ (Cpa3$^{Cre/+}$ BM)) bone marrow.

(B) Gut motility was measured after 90 min of a FITC-dextran gavage for all indicated groups. Data are shown as percent fluorescence of each section of total fluorescence per mouse. Data are from one experiment representative of three independent experiments.

(C) Fasting glucose levels of all aforementioned groups.

(D) Weight gain curves of all four groups when placed on a HFD (n = 4–7).

(E) GTT of all four groups at 14 weeks of HFD feeding (n = 4–7).

(F–H) (F) Total AT mass measured by ECHO-MRI, (G) epididymal AT mass, and (H) total lean mass assessed by ECHO-MRI after 16 weeks of HFD feeding.

Data are shown as mean ± SEM and are from two pooled independent experiments. For all dot plot panels, each dot represents one individual mouse. Statistics were performed as described for Figure 1 above. For all studies bone marrow engraftment of CD117^{+} (*Kit*$^{+/+}$) LSKs was confirmed before inclusion. *p < 0.05; **p < 0.001; ***p < 0.001; ****p < 0.0001 between *Kit*$^{W/Wv}$ mice and their *Kit*$^{+/+}$ and/or *Kit*$^{W/Wv}$ plus BM controls.

Kit$^{W/Wv}$ mouse, in which published metabolic experiments were performed, is on the WBB6F1 background. In this background, we compared *Kit*$^{+/+}$*Cpa3*$^{+/+}$ (*Kit* wild-type, mast cell proficient), *Kit*$^{+/+}$*Cpa3*$^{Cre/+}$ (*Kit* wild-type, mast cell deficient), and *Kit*$^{W/Wv}$ *Cpa3*$^{+/+}$ (*Kit* deficient, mast cell deficient). Mast cell deficiency did not have an impact on the development of obesity, insulin resistance, or T2D in any of these experimental systems.

How could the protection of *Kit*$^{W/Wv}$ and *Kit*$^{W\text{-}sh/W\text{-}sh}$ mice from obesity and insulin resistance be attributed to lack of mast cells? Mice with naturally occurring mutations in the *Kit* locus are mast cell deficient and have been the mainstay of in vivo mast cell research for decades (Nakano et al., 1985). In addition to the well-known pleiotropic defects within the immune system, *Kit* mutations potentially impair metabolically relevant cell lineages or tissue functions including hepatic function (Magnol et al., 2007), insulin secretion from β cells (Feng et al., 2012), and deficiencies in neuronal cells both in the enteric (ICC) and the central nervous system (Huizinga et al., 1995; Maeda et al., 1992; Milenkovic et al., 2007; Takagi et al., 2008). Upon HFD feeding, *Kit*$^{W/Wv}$ mice failed to gain AT mass, had hypertriglyceridemia and low cholesterol levels, and were protected from glucose intolerance and insulin resistance. Our whole-transcriptomic expression profiling revealed that *Kit*-deficient mice fail to enter the normal gene expression program associated in wild-type mice with diet-induced obesity; in fact, gene expression in the AT from *Kit*$^{W/Wv}$ mice on HFD was indistinguishable from normal mice on a LFD. These results underscore the fundamental resistance of *Kit* mutant mice to the pathological response to obesity.

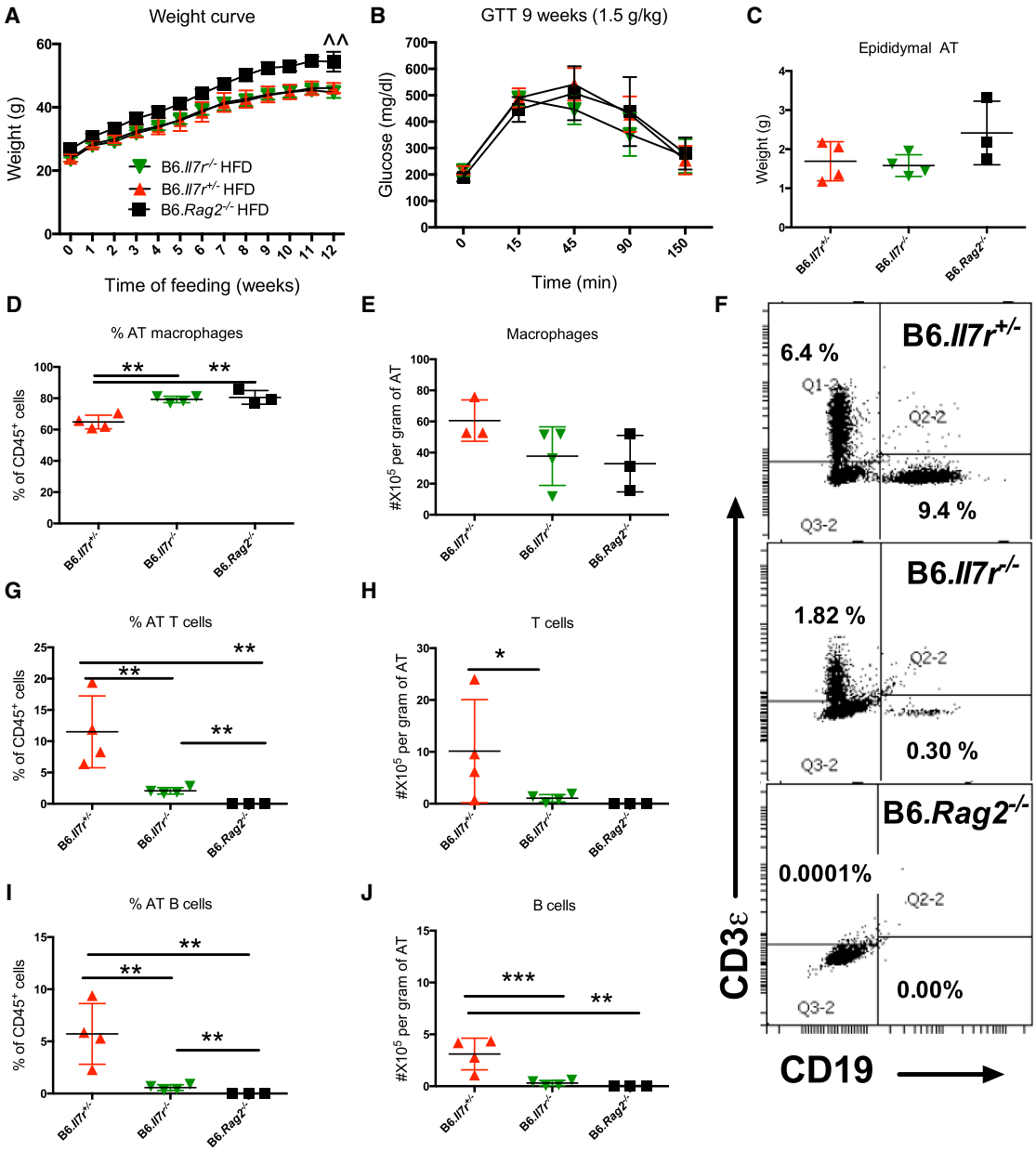

Figure 6. Weight Gain and Glucose Tolerance Are Unaffected by Lymphocyte Deficiency

B6.*Rag2*$^{-/-}$ and B6.*Il7r*$^{-/-}$ mice and B6.*IL7r*$^{+/-}$ controls were placed on a HFD for 12 weeks.

(A) Their weights were tracked weekly for the duration of the study.

(B) GTT after 9 weeks of HFD feeding.

(C–J) Paramaters after 12 weeks of HFD feeding.

(C) Epididymal AT mass.

(D) Percentage of CD45$^+$CD11b$^+$F4/80$^+$ macrophages from total CD45$^+$ cells.

(E) Absolute number of macrophages per gram of AT.

(F) Representative flow cytometric plots of T (CD45$^+$Siglec-F$^-$CD11b$^-$F4/80$^-$CD19$^-$CD3ε$^+$) and B cells (CD45$^+$Siglec-F$^-$CD11b$^-$F4/80$^-$CD3ε$^-$CD19$^+$) in the AT of all indicated groups.

(G) Percentage of T cells from total CD45$^+$ cells.

(H) Absolute number of T cells per gram of AT.

(I) Percentage of B cells from total CD45$^+$ cells.

(J) Absolute number of B cells per gram of AT.

Data are shown as mean ± SEM and are from one experiment with n = 3 to 4 per group. Statistics were performed as described for Figure 1 above. $^{\wedge\wedge}p < 0.01$ between the weight curves of B6.*Rag2*$^{-/-}$ mice and that of B6.*Il7r*$^{-/-}$ and B6.*Il7r*$^{+/-}$ mice. *$p < 0.05$; **$p < 0.01$; ***$p < 0.001$ between the indicated groups.

In recent years, studies in the mast cell field, including the report by Liu et al. (2009), preferred to use $Kit^{W\text{-}sh/W\text{-}sh}$ mice over or in addition to $Kit^{W/Wv}$ mice, mostly due to claims of a "milder" hematopoietic phenotype, a simpler genetic background (C57BL/6), and ease of breeding (Grimbaldeston et al., 2005). However, $Kit^{W\text{-}sh/W\text{-}sh}$ mice, unlike $Kit^{W/Wv}$ mice, which bear point mutations in the *Kit* gene, have a large genomic inversion located upstream of the *Kit* locus that potentially impairs the regulation or function of 28 genes other than *Kit*, including Corin-deficiency-associated cardiomegaly (Nigrovic et al., 2008). In the hematopoetic system, $Kit^{W\text{-}sh/W\text{-}sh}$ mice also display notable defects, including expansion of immature lineage-negative cells, common myeloid progenitors, granulocyte-macrophage progenitors (i.e., evidence for extramedullary myelopoiesis), MDSCs and megakaryocytes in the spleen, and neutrophilia and thrombocytosis in the bone marrow (Michel et al., 2013; Nigrovic et al., 2008). Collectively, key steps in myelopoiesis are defective in $Kit^{W\text{-}sh/W\text{-}sh}$ mice, casting doubt on the usefulness of this mutant for *Kit* studies. Arguably, $Kit^{W/Wv}$ mice are the better-defined model of *Kit* deficiency.

In any case, the protection of *Kit* mutants from obesity and T2D was unrelated to their lack of mast cells, which left open the possibilities that the metabolic phenotype of these mutant mice was due to the Kit-dependent defects within or outside of the immune system. We showed that the protective phenotype of $Kit^{W/Wv}$ mice was immune regulated, as hematopoietic reconstitution with $Kit^{+/+}$ bone marrow into non-irradiated mice reversed this phenotype. The reversal was also achieved by using donor bone marrow that was incompetent to generate mast cells in the $Kit^{W/Wv}$ recipient mice ($Cpa3^{Cre/+}$ HSC), again supporting the mast cell independence of the process. A complementary experiment would be the reconstitution of $Kit^{W/Wv}$ mice with bone-marrow-derived cultured mast cells. However, the concept that mast cell functions are revealed by transplantation of cultured mast cells into *Kit* mutant mice has been shown to be flawed by experiments in new mouse models. Roles for mast cell functions that had been proposed based on the reconstitution system were not reproduced for diverse pathologies, including antibody-driven arthritis, autoimmune encephalitis, wound healing (Antsiferova et al., 2013), or contact hypersensitivity (reviewed in Reber et al., 2012; Peschke et al., 2015). Hence, mast cell reconstitution of *Kit* mutants, considered a pillar of immunology (Kawakami, 2009), turned out to be an unreliable experimental system. This conclusion is clearly underscored here by the fact that, using multiple independent systems, we do not confirm roles for mast cells in protection of *Kit* mutant mice from weight gain and insulin resistance.

This clarification appears important in view of the fact that mast cells have been proposed as a potential therapeutic target against obesity and diabetes (Wang and Shi, 2011). This notion was supported by previous studies showing *Kit*-dependent protection from weight gain and insulin resistance (discussed above) and the promotion of weight loss by daily injections of obese mice with high doses of mast cell stabilizers (Liu et al., 2009; Wang and Shi, 2011; Wang et al., 2013). In the Liu et al. (2009) study, mice were injected daily with 25 mg/kg DSCG or ketotifen; this dose highly exceeds the doses recommended for these drugs in treating asthma and/or allergy in humans by 37.5-fold (DSCG, 40 mg per day) and 750-fold (ketotifen, 2 mg per day), respectively. Despite using comparably high dosages, we were unable to replicate weight loss or prevent weight gain with DSCG. These discrepancies might be explained by off-target effects of mast cell stabilizers (Oka et al., 2012), or by other currently unknown factors including the health status of the mice or different microbiome enterotypes.

Given the complex nature of the hematopoietic lineages and stages that are affected by *Kit* mutations, it remains very challenging to exactly pinpoint the hematopoietic cell type or its dysfunction that underlies the protection of *Kit* mutant mice to obesity and metabolic syndrome. While we excluded classical lymphocytes, including $\alpha\beta$ and $\gamma\delta$ T cells in the small intestine by analysis of diet-induced obesity in *Rag2*- or *Il7r*-deficient mice, other interesting cells affected by *Kit* mutations, notably ILC subsets, have yet to become more accessible for genetic experimentation. As for mast cells, Kit-mediated immunological and non-immunological roles can now be discriminated from those of mast cells by employing mast-cell-specific deficiency mouse models (for detailed considerations, see Katz and Austen, 2011; Peschke et al., 2015; Reber et al., 2012; Rodewald and Feyerabend, 2012). There are several Kit-independent models of mast cell deficiency, both constitutive and inducible (reviewed in Reber et al., 2012), and careful attention must be placed on choosing the appropriate model for the study of choice. In our view, $Cpa3^{Cre/+}$ mice presented the most suitable model for the current study, as it is the only mouse with complete deficiency of both connective and mucosal tissue mast cells without deficiencies in other immune or non-immune compartments, with the exception of a reduction in basophils. Especially in chronic disease models, as in obesity studies, $Cpa3^{Cre/+}$ mice are advantageous over mice with inducible mast cell ablation because the latter require repetitive depletion treatments.

In conclusion, our data showed that obesity, obesity-mediated insulin resistance, and T2D depend on expression of Kit in the hematopoietic system but not outside. Since mast cells are non-essential in the regulation of these diseases, these cells are unlikely to be successful therapeutic targets. However, blockade of other Kit-related hematopoietic functions may serve as potential candidates for the regulation of the metabolic syndrome, as long as they are specific enough not to interfere with basic hematopoietic or immunological functions.

EXPERIMENTAL PROCEDURES

Mice

B6.$Cpa3^{Cre/+}$ mice were obtained after backcrossing the $Cpa3^{Cre}$ allele for >20 generations onto C57BL/6J (B6). In all experiments, littermates from the breeding of B6.$Cpa3^{Cre/+}$ with wild-type B6 mice were used. *Kit* mutant mast-cell-deficient WBB6F1.$Kit^{W/Wv}$ mice and their WBB6F1.$Kit^{+/+}$ littermate controls were obtained by crossing WB.$Kit^{W/+}$ with B6.$Kit^{Wv/+}$ mice. For direct comparison, WBB6F1.$Cpa3^{Cre/+}$ and WBB6F1.$Cpa3^{+/+}$ littermates were generated in crosses of WB.$Kit^{+/+}$ with B6.$Cpa3^{Cre/+}$ mice. B6.$Lep^{Ob/Ob}$ $Cpa3^{Cre/+}$ mice and their littermate controls were generated by crossing B6.$Lep^{Ob/+}$ with B6.$Cpa3^{Cre/+}$ mice and intercrossing the F1 generation. B6.$Il7^{-/-}$ and their littermate B6.$Il7^{+/-}$ controls were obtained by intercrossing B6.$Il7^{+/-}$ mice. B6.$Rag2^{-/-}$ were maintained as homozygous knockouts. All animals were generated at the mouse breeding facilities of the DKFZ in Heidelberg. All experiments were conducted in accordance to animal care guidelines

pertaining to local animal committees (Regierungspräsidium Karlsruhe) and to the institutional guidelines (DKFZ, Heidelberg).

Animal Feeding

Experimental animals were maintained with ad libitum access to food and water. All feeding studies were started with 8-week-old male or female mice. Experimental diets were either a HFD (60% kcal from fat; 35% fat content, Research Diets, Inc.; order number D12492) or LFD (6% crude fat content, Kliba Nafag; order number 3302). The B6.*Lep*$^{Ob/Ob}$*Cpa3*$^{Cre/+}$ mice and their littermate controls were always kept on the 6% fat LFD.

Bone Marrow Transplantation

For bone marrow reconstitutions, 6-week-old non-irradiated WBB6F1.*Kit*$^{W/Wv}$ male mice were transplanted intravenously with 2 × 10^6 total bone marrow cells from WBB6F1.*Cpa3*$^{Cre/+}$ or WBB6F1.*Kit*$^{+/+}$ donors. Only the animals that were tested positive for donor chimerism (hematocrit $\geq$ 45%) 6 weeks after transplantation were used for further experiments.

DSCG Treatment

Male 8-week-old mice were placed on a HFD and injected intraperitoneally daily with a 25 mg/kg dose DSCG or saline for 7 weeks. Their weights were tracked weekly for the duration of the study.

Body Weight and Composition

Body weight was measured weekly for the duration of the studies. Total lean mass, AT mass, and free fluid composition were measured by magnetic resonance imaging using an Echo-MRI-100 system after 8, 12, or 16 weeks of feeding and after 22 weeks of age for the B6.*Lep*$^{Ob/Ob}$*Cpa3*$^{Cre/+}$ study.

Tissue Collection

After 8 or 16 weeks of feeding or 22 weeks of age, mice were fasted for 5 hr starting at 7:00 AM and injected intraperitoneally with insulin (1U per kg body weight of Huminsulin, Eli Lilly) or saline, 15 min prior to euthanasia. Liver, gastrocnemius muscle, epididymal AT, perirenal AT, spleen, kidneys, and pancreas were collected post-PBS perfusion. The collected organs were weighed and distributed for further RNA isolation (stored in RNA later, QIAGEN), protein extraction (cryofreezing), and formalin-fixed for histological sectioning and staining.

Protein Purification and Western Blot Analysis

Frozen tissue was homogenized in RIPA lysis buffer for protein extraction. The amount of protein in the lysates was measured using the BCA Protein quantification kit (Thermo Scientific). Quantified protein was used for western blot analysis with antibodies against mouse Akt (clone C67E7), mouse phospho-Akt (Ser 473) (clone D9E), and β-actin (clone 13E5), all from Cell Signaling Technology, Inc. The band intensities were quantified using ImageJ software.

Histological Examination of Mast Cells

Portions of the harvested and weighed gastrocnemius muscle and epididymal AT were formalin-fixed and paraffin-embedded. Tissue was cut into 5 μm sections and stained with 0.1% w/v toluidine blue O stain (Sigma). Portions of liver tissue were preserved in Tissue-tek O.C.T compound (Sakura), and 6 μm cryostat sections were made. Liver sections were stained with 0.1% w/v toluidine blue O stain. Images were taken using a Zeiss Axioplan light microscope at 200× magnification.

RNA Isolation and qRT-PCR

Liver, gastrocnemius muscle, and epididymal AT were used for RNA purification using RNeasy Plus Universal Mini kit (QIAGEN, from muscle) and RNeasy Plus Mini kit (QIAGEN, from liver and epididymal AT) following manufacturer's instructions. Isolated RNA was quantified using the NanoDrop 2000c UV-Vis Spectrophotometer (Thermo Scientific). cDNA synthesis was carried out with 400 ng total RNA using the High Capacity cDNA Reverse Transcription kit (Applied Biosystems), following manufacturer's instructions. Real-time PCR was performed using the ViiA 7 Real-Time PCR System (Applied Biosystems). Reactions were carried out using TaqMan Fast Advanced Master Mix (Applied Biosystems). Gene probes used include *Emr1* (Mm00802529_m1), *Cpa3* (Mm00483940_m1), *Tnf* (Mm00443258_m1), *Gapdh* (Mm99999915_g1), *Ccl2* (Mm00441242_m1), *Il6* (Mm00446190_m1), and *Cma1* (Mm00487638_m1). The data were analyzed using the Pfaffel method, and *Gapdh* expression was used as the housekeeping gene.

AT Microarray

Total RNA was isolated from epididymal AT and used for microarray analysis using an Illumina Whole-Genome BeadChip Sentrix mouse WG-6 v2 array. Data were analyzed using the chipster platform and normalized with the quantile normalization method. The accession number for the microarray data reported in this paper is GEO: GSE67091.

GTT and Hematocrit Analysis

Tail vein blood was used for hematocrit analyses using heparinized micro-hematocrit capillary tubes and a Thermo scientific capillary centrifuge with micro-hematocrit scale. Tail vein blood glucose levels were measured in 8-week-old mice, prior to being designated to their respective diet groups or 6 weeks after bone marrow transplantation. After 6 or 14 weeks of being fed their designated diets, or 19 weeks of age for the B6.*Lep*$^{Ob/Ob}$*Cpa3*$^{Cre/+}$ study, GTTs were performed on mice that were fasted for 5 hr before baseline blood glucose measurement. This was followed by intraperitoneal injection of glucose (0.5 g per kg of body mass) and subsequent measurement of blood glucose at 15, 30, 45, 60, 90, and 150 min time points.

Plasma Metabolite Measurement

For isolation of blood plasma, approximately 200 μl of blood were collected from the superficial temporal vein in EDTA-filled tubes (6 μl of 500 mM EDTA per tube). The sampled blood was centrifuged at 13,000 rpm for 20 min at 4°C, and the blood plasma was separated and stored at −80°C for further analysis. Insulin levels of blood plasma were assessed using ELISA (Rat/Mouse Insulin 96 Well Plate Assay, EMD Millipore), following the manufacturer's instructions. Blood plasma was used for cholesterol quantification using the Total Cholesterol Assay Kit (Cell Biolabs) following manufacturer's instructions. Plasma triglycerides were quantified using the colorimetric Serum Triglycerides Quantification Kit (Cell Biolabs) following the manufacturer's instructions.

Stromal Vascular Fraction Isolation and Flow Cytometry

Freshly isolated epididymal AT was weighed, and 0.5 g of AT were digested for 30 min with 1 mg/ml collagenase VIII (Sigma-aldrich) at 37°C under constant shaking (200 rpm). The immune-cell-containing stromal vascular fraction was separated from the adipocyte fraction by centrifugation and used for flow cytometry analysis. Stromal vascular fraction cells and whole bone marrow cells were incubated with total mouse IgG (0.283 mg/ml) (Jackson ImmunoResearch Laboratories, Inc) for 20 min for Fc blocking. Cells were then incubated for 45 min with an antibody cocktail mix, discriminative for the indicated immune cells: mast cells (CD45$^+$CD117$^+$IgE$^+$F4/80$^-$), eosinophils (CD45$^+$CD11b^{low}F4/80^{low}SiglecF$^+$), macrophages (CD45$^+$CD11b$^+$F4/80$^+$ SiglecF$^-$), CD4$^+$ T cells (CD3$^+$CD4$^+$), CD8$^+$ T cells (CD3$^+$CD8α$^+$), Treg (CD3$^+$CD4$^+$Foxp3$^+$), B cells (CD19$^+$CD3$^-$), and LSKs Lin$^-$ (CD3, CD4, CD8, CD19, Ter119, Gr1, NK1.1, CD11b, and CD11c), and CD117$^+$Sca-1$^+$ cells. The specific clones and fluorochromes utilized for FACS experiments are listed in Table S1.

Gut Motility Assay

Mice were fasted individually for 90 min in empty mouse cages. After the fast, water was removed and 15 μl of 70 kDa FITC-labeled dextran (6.25 mg/ml in 0.9% saline) was given to the mice via oral gavage. 90 min later, mice were euthanized by CO_2 asphyxiation, and the GI tract was removed by a subdiaphragmal transection of the esophagus and the colon at the most distal position. The GI tract was then divided into 15 fractions, paying careful attention to avoid movement of intestinal contents; the fractions were divided into stomach, ten equally sized small intestine fractions, caecum, and three equally sized colon fragments. The content of each fraction was collected into ice-cold Krebs buffer, and fluorescence intensity in each fraction was measured using a fluorescence plate reader at 485/528 nm excitation/emission.

Statistical Analysis

Graph Pad Prism software was used for plotting data and for statistical analysis (Graph Pad Software). Unpaired Student's t test and one-way ANOVA

were used to evaluate statistical significance. Values of $p < 0.05$ were considered statistically significant. Statistical significance of data sets that consisted of more than two variables was analyzed using two-way ANOVA analysis. Data are presented as mean ± SEM unless noted otherwise.

SUPPLEMENTAL INFORMATION

Supplemental Information includes four figures and one table and can be found with this article online at http://dx.doi.org/10.1016/j.cmet.2015.04.013.

AUTHOR CONTRIBUTIONS

D.A.G. designed and performed the experiments, analyzed the data, and wrote the manuscript. S.M. performed experiments. T.B.F. contributed to mouse generation and edited the manuscript. S.H. contributed to experimental design and provided intellectual and material support. H.-R.R. contributed to experimental design and co-wrote/edited the manuscript.

ACKNOWLEDGMENTS

The authors would like to thank Ann-Kathrin Schuon, Sofia Santamaria, Anna-Lena Geiselhöringer, Tabea Arnsperger, and Sven Schaefer from the Division of Cellular Immunology (DKFZ) for expert technical assistance; the animal facility at the DKFZ for expert mouse husbandry; and Tatjana Schmidt, Microarray Unit, Genomics and Proteomics Core Facility at DKFZ, for expression array experiments. Additionally, we would like to thank Gianluca Matteoli at KU Leuven for providing advice on the gut motility study. D.A.G. was initially funded by a DKFZ postdoctoral fellowship. H.-R.R. was funded by the European Research Council advanced grant 233074. S.H. was funded by the Deutsche Forschungsgemeinschaft (He3260/8-1) and the Helmholtz ICEMED Alliance. The authors declare no conflicts of interest associated with this article.

Received: December 22, 2014
Revised: February 20, 2015
Accepted: April 7, 2015
Published: May 5, 2015

REFERENCES

Altintas, M.M., Azad, A., Nayer, B., Contreras, G., Zaias, J., Faul, C., Reiser, J., and Nayer, A. (2011). Mast cells, macrophages, and crown-like structures distinguish subcutaneous from visceral fat in mice. J. Lipid Res. *52*, 480–488.

Antsiferova, M., Martin, C., Huber, M., Feyerabend, T.B., Förster, A., Hartmann, K., Rodewald, H.R., Hohl, D., and Werner, S. (2013). Mast cells are dispensable for normal and activin-promoted wound healing and skin carcinogenesis. J. Immunol. *191*, 6147–6155.

Chappaz, S., Gärtner, C., Rodewald, H.R., and Finke, D. (2010). Kit ligand and Il7 differentially regulate Peyer's patch and lymph node development. J. Immunol. *185*, 3514–3519.

Divoux, A., Moutel, S., Poitou, C., Lacasa, D., Veyrie, N., Aissat, A., Arock, M., Guerre-Millo, M., and Clément, K. (2012). Mast cells in human adipose tissue: link with morbid obesity, inflammatory status, and diabetes. J. Clin. Endocrinol. Metab. *97*, E1677–E1685.

Dudeck, A., Dudeck, J., Scholten, J., Petzold, A., Surianarayanan, S., Köhler, A., Peschke, K., Vöhringer, D., Waskow, C., Krieg, T., et al. (2011). Mast cells are key promoters of contact allergy that mediate the adjuvant effects of haptens. Immunity *34*, 973–984.

Eheim, A., Medrikova, D., and Herzig, S. (2014). Immune cells and metabolic dysfunction. Semin. Immunopathol. *36*, 13–25.

Feng, Z.C., Li, J., Turco, B.A., Riopel, M., Yee, S.P., and Wang, R. (2012). Critical role of c-Kit in beta cell function: increased insulin secretion and protection against diabetes in a mouse model. Diabetologia *55*, 2214–2225.

Feyerabend, T.B., Weiser, A., Tietz, A., Stassen, M., Harris, N., Kopf, M., Radermacher, P., Möller, P., Benoist, C., Mathis, D., et al. (2011). Cre-mediated cell ablation contests mast cell contribution in models of antibody- and T cell-mediated autoimmunity. Immunity *35*, 832–844.

Gomez-Pinilla, P.J., Farro, G., Di Giovangiulio, M., Stakenborg, N., Némethova, A., de Vries, A., Liston, A., Feyerabend, T.B., Rodewald, H.R., Boeckxstaens, G.E., and Matteoli, G. (2014). Mast cells play no role in the pathogenesis of postoperative ileus induced by intestinal manipulation. PLoS ONE *9*, e85304.

Gordon, J.R., and Galli, S.J. (1990). Mast cells as a source of both preformed and immunologically inducible TNF-alpha/cachectin. Nature *346*, 274–276.

Grimbaldeston, M.A., Chen, C.C., Piliponsky, A.M., Tsai, M., Tam, S.Y., and Galli, S.J. (2005). Mast cell-deficient W-sash c-kit mutant Kit W-sh/W-sh mice as a model for investigating mast cell biology in vivo. Am. J. Pathol. *167*, 835–848.

Gutierrez, D.A., Fu, W., Schonefeldt, S., Feyerabend, T.B., Ortiz-Lopez, A., Lampi, Y., Liston, A., Mathis, D., and Rodewald, H.R. (2014). Type 1 diabetes in NOD mice unaffected by mast cell deficiency. Diabetes *63*, 3827–3834.

Hill, A.A., Reid Bolus, W., and Hasty, A.H. (2014). A decade of progress in adipose tissue macrophage biology. Immunol. Rev. *262*, 134–152.

Hotamisligil, G.S., and Erbay, E. (2008). Nutrient sensing and inflammation in metabolic diseases. Nat. Rev. Immunol. *8*, 923–934.

Hotamisligil, G.S., Arner, P., Caro, J.F., Atkinson, R.L., and Spiegelman, B.M. (1995). Increased adipose tissue expression of tumor necrosis factor-alpha in human obesity and insulin resistance. J. Clin. Invest. *95*, 2409–2415.

Huizinga, J.D., Thuneberg, L., Klüppel, M., Malysz, J., Mikkelsen, H.B., and Bernstein, A. (1995). W/kit gene required for interstitial cells of Cajal and for intestinal pacemaker activity. Nature *373*, 347–349.

Ishii, S., Tsuji, S., Tsujii, M., Nishida, T., Watabe, K., Iijima, H., Takehara, T., Kawano, S., and Hayashi, N. (2009). Restoration of gut motility in Kit-deficient mice by bone marrow transplantation. J. Gastroenterol. *44*, 834–841.

Katz, H.R., and Austen, K.F. (2011). Mast cell deficiency, a game of kit and mouse. Immunity *35*, 668–670.

Kawakami, T. (2009). A crucial door to the mast cell mystery knocked in. J. Immunol. *183*, 6861–6862.

Kiss, E.A., Vonarbourg, C., Kopfmann, S., Hobeika, E., Finke, D., Esser, C., and Diefenbach, A. (2011). Natural aryl hydrocarbon receptor ligands control organogenesis of intestinal lymphoid follicles. Science *334*, 1561–1565.

Kitamura, Y., Yokoyama, M., Matsuda, H., and Shimada, M. (1980). Coincidental development of forestomach papilloma and prepyloric ulcer in nontreated mutant mice of W/Wv and Sl/Sld genotypes. Cancer Res. *40*, 3392–3397.

Liu, J., Divoux, A., Sun, J., Zhang, J., Clément, K., Glickman, J.N., Sukhova, G.K., Wolters, P.J., Du, J., Gorgun, C.Z., et al. (2009). Genetic deficiency and pharmacological stabilization of mast cells reduce diet-induced obesity and diabetes in mice. Nat. Med. *15*, 940–945.

Maeda, H., Yamagata, A., Nishikawa, S., Yoshinaga, K., Kobayashi, S., Nishi, K., and Nishikawa, S. (1992). Requirement of c-kit for development of intestinal pacemaker system. Development *116*, 369–375.

Magnol, L., Chevallier, M.C., Nalesso, V., Retif, S., Fuchs, H., Klempt, M., Pereira, P., Riottot, M., Andrzejewski, S., Doan, B.T., et al. (2007). KIT is required for hepatic function during mouse post-natal development. BMC Dev. Biol. *7*, 81.

Mathis, D. (2013). Immunological goings-on in visceral adipose tissue. Cell Metab. *17*, 851–859.

McNelis, J.C., and Olefsky, J.M. (2014). Macrophages, immunity, and metabolic disease. Immunity *41*, 36–48.

Michel, A., Schüler, A., Friedrich, P., Döner, F., Bopp, T., Radsak, M., Hoffmann, M., Relle, M., Distler, U., Kuharev, J., et al. (2013). Mast cell-deficient Kit(W-sh) "Sash" mutant mice display aberrant myelopoiesis leading to the accumulation of splenocytes that act as myeloid-derived suppressor cells. J. Immunol. *190*, 5534–5544.

Milenkovic, N., Frahm, C., Gassmann, M., Griffel, C., Erdmann, B., Birchmeier, C., Lewin, G.R., and Garratt, A.N. (2007). Nociceptive tuning by stem cell factor/c-Kit signaling. Neuron *56*, 893–906.

Mraz, M., and Haluzik, M. (2014). The role of adipose tissue immune cells in obesity and low-grade inflammation. J. Endocrinol. *222*, R113–R127.

Nakano, T., Sonoda, T., Hayashi, C., Yamatodani, A., Kanayama, Y., Yamamura, T., Asai, H., Yonezawa, T., Kitamura, Y., and Galli, S.J. (1985). Fate of bone marrow-derived cultured mast cells after intracutaneous, intraperitoneal, and intravenous transfer into genetically mast cell-deficient W/Wv mice. Evidence that cultured mast cells can give rise to both connective tissue type and mucosal mast cells. J. Exp. Med. *162*, 1025–1043.

Nigrovic, P.A., Gray, D.H., Jones, T., Hallgren, J., Kuo, F.C., Chaletzky, B., Gurish, M., Mathis, D., Benoist, C., and Lee, D.M. (2008). Genetic inversion in mast cell-deficient (Wsh) mice interrupts corin and manifests as hematopoietic and cardiac aberrancy. Am. J. Pathol. *173*, 1693–1701.

Oka, T., Kalesnikoff, J., Starkl, P., Tsai, M., and Galli, S.J. (2012). Evidence questioning cromolyn's effectiveness and selectivity as a 'mast cell stabilizer' in mice. Lab. Invest. *92*, 1472–1482.

Peschke, K., Dudeck, A., Rabenhorst, A., Hartmann, K., and Roers, A. (2015). Cre/loxP-based mouse models of mast cell deficiency and mast cell-specific gene inactivation. Methods Mol. Biol. *1220*, 403–421.

Piconese, S., Costanza, M., Musio, S., Tripodo, C., Poliani, P.L., Gri, G., Burocchi, A., Pittoni, P., Gorzanelli, A., Colombo, M.P., and Pedotti, R. (2011). Exacerbated experimental autoimmune encephalomyelitis in mast-cell-deficient Kit W-sh/W-sh mice. Lab. Invest. *91*, 627–641.

Puddington, L., Olson, S., and Lefrançois, L. (1994). Interactions between stem cell factor and c-Kit are required for intestinal immune system homeostasis. Immunity *1*, 733–739.

Reber, L.L., Marichal, T., and Galli, S.J. (2012). New models for analyzing mast cell functions in vivo. Trends Immunol. *33*, 613–625.

Rodewald, H.R., and Feyerabend, T.B. (2012). Widespread immunological functions of mast cells: fact or fiction? Immunity *37*, 13–24.

Russell, E.S. (1979). Hereditary anemias of the mouse: a review for geneticists. Adv. Genet. *20*, 357–459.

Schönhuber, N., Seidler, B., Schuck, K., Veltkamp, C., Schachtler, C., Zukowska, M., Eser, S., Feyerabend, T.B., Paul, M.C., Eser, P., et al. (2014). A next-generation dual-recombinase system for time- and host-specific targeting of pancreatic cancer. Nat. Med. *20*, 1340–1347.

Sergeant, G.P., Large, R.J., Beckett, E.A., McGeough, C.M., Ward, S.M., and Horowitz, B. (2002). Microarray comparison of normal and W/Wv mice in the gastric fundus indicates a supersensitive phenotype. Physiol. Genomics *11*, 1–9.

Shimada, M., Kitamura, Y., Yokoyama, M., Miyano, Y., Maeyama, K., Yamatodani, A., Takahashi, Y., and Tatsuta, M. (1980). Spontaneous stomach ulcer in genetically mast-cell depleted W/Wv mice. Nature *283*, 662–664.

Takagi, K., Okuda-Ashitaka, E., Mabuchi, T., Katano, T., Ohnishi, T., Matsumura, S., Ohnaka, M., Kaneko, S., Abe, T., Hirata, T., et al. (2008). Involvement of stem cell factor and its receptor tyrosine kinase c-kit in pain regulation. Neuroscience *153*, 1278–1288.

Tanaka, A., Nomura, Y., Matsuda, A., Ohmori, K., and Matsuda, H. (2011). Mast cells function as an alternative modulator of adipogenesis through 15-deoxy-delta-12, 14-prostaglandin J2. Am. J. Physiol. Cell Physiol. *301*, C1360–C1367.

Uysal, K.T., Wiesbrock, S.M., Marino, M.W., and Hotamisligil, G.S. (1997). Protection from obesity-induced insulin resistance in mice lacking TNF-alpha function. Nature *389*, 610–614.

Wang, J., and Shi, G.P. (2011). Mast cell stabilization: novel medication for obesity and diabetes. Diabetes Metab. Res. Rev. *27*, 919–924.

Wang, J., Sjöberg, S., Tia, V., Secco, B., Chen, H., Yang, M., Sukhova, G.K., and Shi, G.P. (2013). Pharmaceutical stabilization of mast cells attenuates experimental atherogenesis in low-density lipoprotein receptor-deficient mice. Atherosclerosis *229*, 304–309.

Waskow, C., and Rodewald, H.R. (2002). Lymphocyte development in neonatal and adult c-Kit-deficient (c-KitW/W) mice. Adv. Exp. Med. Biol. *512*, 1–10.

Waskow, C., Paul, S., Haller, C., Gassmann, M., and Rodewald, H.R. (2002). Viable c-Kit(W/W) mutants reveal pivotal role for c-kit in the maintenance of lymphopoiesis. Immunity *17*, 277–288.

Waskow, C., Madan, V., Bartels, S., Costa, C., Blasig, R., and Rodewald, H.R. (2009). Hematopoietic stem cell transplantation without irradiation. Nat. Methods *6*, 267–269.

Willenborg, S., Eckes, B., Brinckmann, J., Krieg, T., Waisman, A., Hartmann, K., Roers, A., and Eming, S.A. (2014). Genetic ablation of mast cells redefines the role of mast cells in skin wound healing and bleomycin-induced fibrosis. J. Invest. Dermatol. *134*, 2005–2015.

Zhou, J.S., Xing, W., Friend, D.S., Austen, K.F., and Katz, H.R. (2007). Mast cell deficiency in Kit(W-sh) mice does not impair antibody-mediated arthritis. J. Exp. Med. *204*, 2797–2802.